Supporting Information

Elucidation of $CuWO_4$ Surface States During Photoelectrochemical Water Oxidation

Yuan Gao and Thomas W. Hamann*
Michigan State University, Department of Chemistry
578 S Shaw Lane East Lansing, Michigan 48824-1322, United States

Corresponding Author

*hamann@chemistry.msu.edu

Experimental

Film Preparation and Characterization

1) $CuWO_4$ by Atomic Layer Deposition

Copper tungstate ($CuWO_4$) thin films were deposited on fluorine-doped tin oxide (FTO) coated glass (Hartford Glass, 12 Ω cm^{-2}) and Si wafer (University Wafer) by an atomic layer stack deposition-annealing (SDA) method (Savannah 100, Cambridge Nanotech Inc.) using a procedure described previously.[1] Briefly, the substrates were sonicated in soap water, distilled water and isopropanol, and blown dry with nitrogen prior to deposition. The precursors for the deposition of WO_3 and CuO were bis(*tert*-butylimido)bis(dimethylamido)tungsten (VI) (Strem Chemicals Inc., >97%) and *N,N'*-di-*sec*-butylacetamidinate (Dow Chemical Co., >99.0%), respectively. The nitrogen carrier gas was kept at 5 sccm. 1000 ALD cycles of WO_3 was deposited using a modified version of a reported procedure.[2] The tungsten precursor was heated up to 75 °C. In each ALD cycle, the tungsten precursor was pulsed for 2 s, followed by 10 s under exposure mode and 6 s nitrogen purge. De-ionized water (millipore, 18 MΩm) was used as the oxidant and was pulsed for 0.5 s followed by 15 s of exposure mode and 6 s of purge. ~170 ALD cycles of CuO was deposited on 1000 cycles of WO_3 according to calculations described in our previous work[1] to match 1:1 ratio between the two metals. The copper precursor was heated to 150 °C and was pulsed for 3 s in each ALD cycle. After purging for 6 s, the oxidation was performed. The oxidation was a 2 s ozone (~10% by weight O_3 in ultrahigh purity O_2 produced by Yanco Industries ozone generator) pulse, followed by a 3 s purge to allow for enough generation of ozone, and performed for 10 times. After deposition, the stack of binary oxides was annealed at 550 °C in air for 30 min with a ramping rate of 2 °C / min. The thickness of as-deposited WO_3 films were measured to be ~65 nm thick on Si by ellipsometry measurements (Horiba Jobin Yvon, Smart-SE) and the thickness of the $CuWO_4$ thin film was calculated to be ~80 nm[1].

2) $CuWO_4$ by spray pyrolysis (SP-$CuWO_4$)

$CuWO_4$ was also synthesized by spray pyrolysis using a modified procedure from literature.[3] An aqueous precursor solution containing 0.01 M of Cu (II) and 0.01 M of W (II) was prepared from $CuCl\bullet 2H_2O$ and $(NH_4)_6H_2W_{12}O_{40}\bullet 4H_2O$. FTO coated glass substrate was kept at 275 °C at a distance of 31 cm from the nozzle. The precursor solution was sprayed onto the substrate for 1 s and the wait time was 5 s. The as-deposited film was then annealed at 550 °C in air for 1 hr with 1 hr ramping time. The composition and structure of the resulted film was characterized using Raman spectroscopy (LabRam Armis, Horiba Jobin Yvon, 532 nm laser, ×50 microscope) and X-ray diffraction (Bruker Davinci Diffractometer operating at 40 kV and 40 mA using Cu Kα radiation). The thickness of the resulted film was determined to be 2 µm by cross-section scanning electron microscopy (SEM) (Carl Zeiss Microscopy).

Measurements in Aqueous Electrolytes

$CuWO_4$ electrodes measured in aqueous electrolytes were masked with a 60 µm Surlyn film (Solaronix) with a 0.28 cm^2 hole to define the active area and to prevent scratching of the thin films. The electrodes were clamped to a custom-made glass electrochemical cell with a quartz window to allow illumination from the electrolyte-electrode (front) side. Surlyn films were adhered to the electrodes by heating to 120 °C. A home-made “no leak” saturated Ag/AgCl electrode was used as a reference electrode in aqueous electrolytes, and high surface area platinum mesh was used as the counter electrode. The working electrodes were examined in contact with aqueous pH 9.0 1 M KB_i buffer with or without 0.5 M Na_2SO_3. The 1 M KB_i buffer was prepared by adding an appropriate amount of KOH pellets into 1 M H_3BO_3 to adjust the pH. The pH was determined using a Fisher Scientific Accumet pH meter. All potentials measured in aqueous solutions were converted to the reversible hydrogen electrode (RHE) scaled by the equation $V_{RHE} = V_{Ag/AgCl} + 0.197 + \mathrm{pH}(0.059)$.

Measurements in Non-aqueous Electrolytes

When in contact with a non-aqueous electrolyte, no Surlyn film was used thus the surface area was defined by the o-ring which is 0.64 cm^2. A custom-made glass electrochemical cell without a quartz window was used in the case of a non-aqueous electrolyte to avoid dissolution of the glue. 0.01M $Ag/AgNO_3$ was dissolved in acetonitrile (MeCN) with 0.1 M tetrabutylammonium hexafluorophosphate ($TBAPF_6$) as the reference electrode. The working electrodes were examined in contact with anhydrous MeCN or dichloromethane with 0.2 M $TBAPF_6$ as the supporting electrolyte. Measurements in anhydrous solutions were conducted in the glove box.

Electrochemical / Photoelectrochemical Measurements

All photoelectrochemical measurements were made with an Eco Chemie Autolab potentiostat coupled with Nova electrochemical software. Current density-voltage (*J*-*V*) curves were measured using a scan rate of 20 mV s^{-1}. The white light source was a 450 W Xe arc lamp (Horiba Jobin Yvon). An AM 1.5 solar filter was used to simulate sunlight at 100 mW cm^{-2}. A neutral density filter was used to reduce the light intensity to 10 mW cm^{-2}. All photoelectrochemical measurements in aqueous solutions were performed by shining light on the $CuWO_4$ electrode through the electrolyte. Photocurrent densities (J_{photo}) were obtained by subtracting the dark current density (J_{dark}) from the total current density under illumination (J_{total}).

Cyclic voltammogram (CV) surface state measurements were performed by applying a positive potential under 1 sun illumination or in the dark for 60 seconds, and then scanning toward the cathodic direction over a potential range in the dark.

EIS data were gathered using a 10 mV amplitude perturbation of between 10000 and 0.04 Hz in the dark or under illumination of 0.1 sun or 1 sun. Neutral density filters were used to adjust the intensity to 10 mW cm^{-2} (0.1 sun). Data were fitted using Zview software (Scribner Associates).

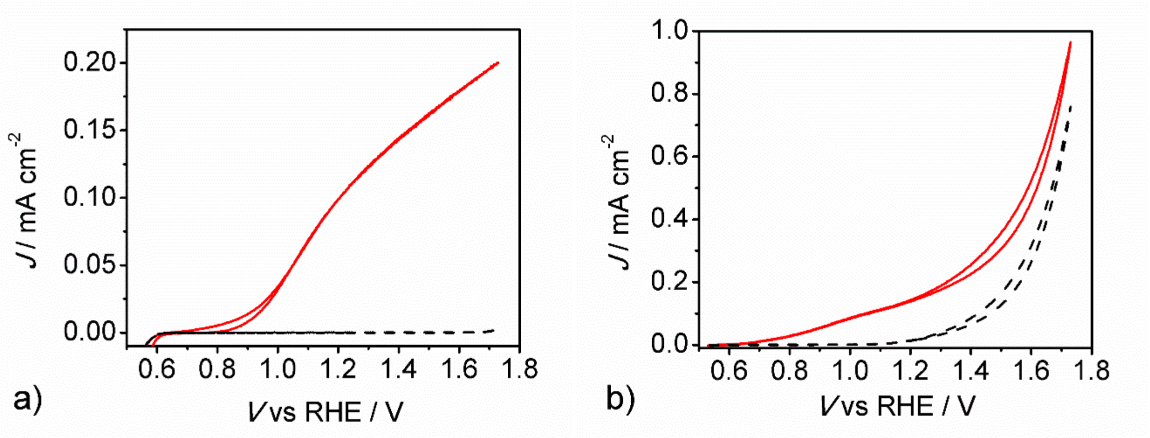

Figure S1. J_{dark}-V (black dash) and J_{total}-V (red solid) curves of $CuWO_4$ electrode measured in a) H_2O and b) 0.5 M Na_2SO_3 electrolytes in the dark and under 1 sun illumination.

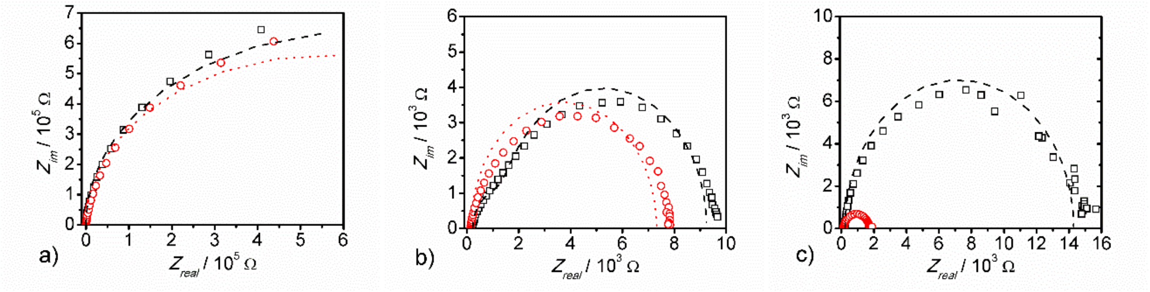

Figure S2. Nyquist plots of $CuWO_4$ electrode at 0.93 V vs RHE a) in the dark and b) under 1 sun illumination and c) at 1.53 V vs RHE under 1 sun illumination. Data measured in H_2O (black squares) and 0.5 M Na_2SO_3 (red circles) are both shown. Fitting curves are shown as black dash for H_2O and red dots for Na_2SO_3.

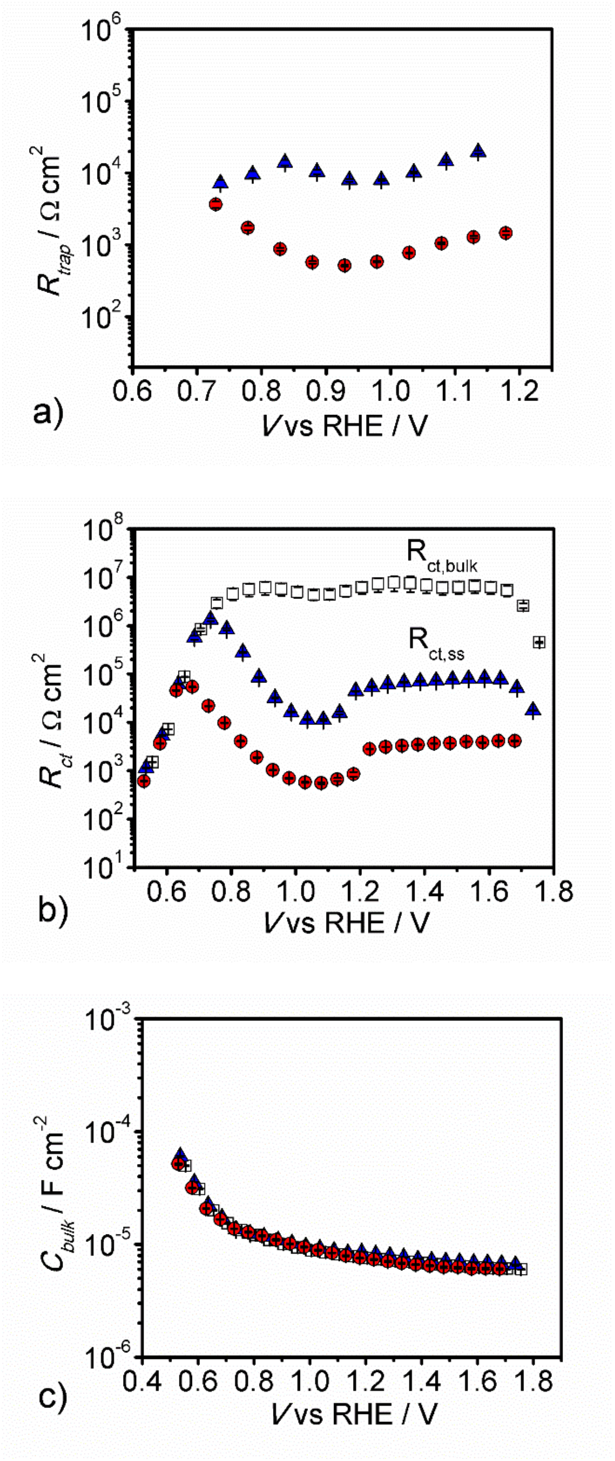

Figure S3. Plots of equivalent circuit parameters obtained from fitting EIS data in the dark (open squares), under 0.1 sun (blue triangles) and 1 sun (red circles) illumination in H_2O electrolyte. a) Resistance of trapping of holes in surface states; b) Charge transfer resistance; c) Bulk capacitance.

Calculation of Mott-Schottky plots:

The flat band potential, V_{fb}, and the dopant density, N_D, can be calculated from the following equation:

$$C_{bulk}^{-2} = \frac{2}{q\varepsilon\varepsilon_0 N_D}\left(V - V_{fb} - \frac{kT}{q}\right) \tag{1}$$

where q is the elementary charge (1.6×10^{-19} C), ε is the dielectric constant of $CuWO_4$ (83)[4], ε_0 is the vacuum permittivity (8.854×10^{-12} F m^{-1}), V is the applied potential, k is the Boltzmann constant (1.38×10^{23} m^2 kg s^{-2} K^{-1}), T is the room temperature (300 K).

Illumination / sun	**V_{fb} / V vs RHE**	**N_d / cm^{-3}**
0	0.50 ± 0.02	$6.3\ (\pm 0.1) \times 10^{19}$
0.1	0.47 ± 0.04	$8.0\ (\pm 0.3) \times 10^{19}$
1	0.51 ± 0.02	$6.7\ (\pm 0.1) \times 10^{19}$

Table S1. Flat band potential and dopant density calculated from Mott-Schottky plots in the dark and under illumination.

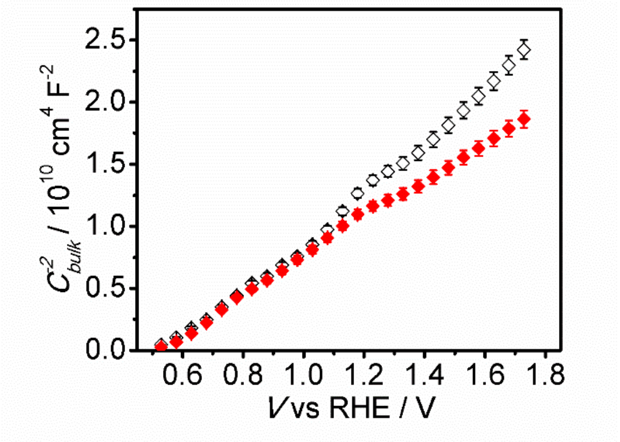

Figure S4. Mott-Schottky plots of $CuWO_4$ immersed in aqueous electrolyte with 0.5 M Na_2SO_3, measured in the dark (open squares) and under 1 sun (red circles) illumination.

Current transient measurements were taken on $CuWO_4$ to study the charge storage behavior of its surface states. Figure S5a shows that a spike in current appears upon turning the light on, which decays quickly to a lower steady state current. This indicates that upon illumination, photogenerated holes accumulate at the surface, resulting in the initial transient current. Afterwards, only a portion of these photogenerated holes undergo charge transfer (water oxidation) at the electrode/electrolyte interface, which contributes to the steady state photocurrent. When the light is switched off, as in Figure S5b, the accumulated holes at the surface recombine with CB electrons, which causes the cathodic spike, and eventually the current reaches its steady state level (dark current). We note that the scale of the transient current first increases with potential, and after it reaches a maximum level, it decreases with potential. Each cathodic transient current is integrated in order to calculate the charge stored in the surface state. The Gaussian behavior of the charge as a function of potential shown in Figure S5c agrees well with the behavior of a chemical capacitance.[5,6] Interestingly, the peak of accumulated charge appears around 1.0 V vs RHE, which is at the same potential as C_{ss} peak in EIS measurements. This confirms that the second capacitive feature observed in EIS measurements is related to the charging of the surface state of $CuWO_4$.

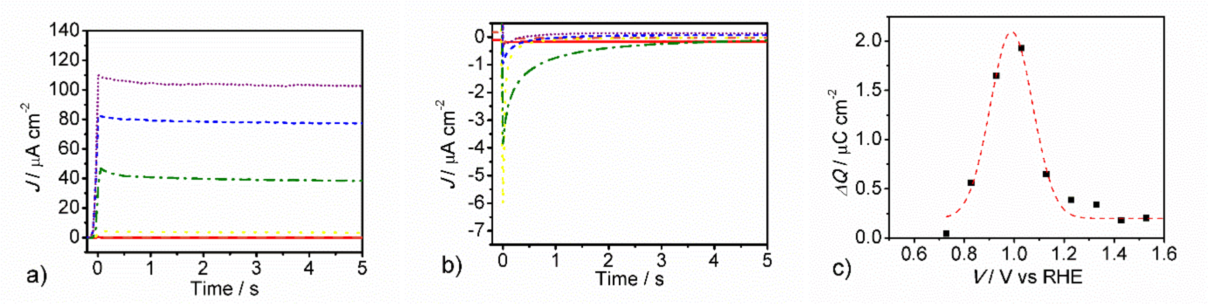

Figure S5. Current transients of $CuWO_4$ in H_2O after turning the 1 sun illumination a) on and b) off. The applied potential varies from 0.68, 0.73, 0.83, 1.03, 1.23 and 1.43 V vs RHE corresponding to red solid, orange dash, yellow dots, green dash dots, blue short dash and purple short dots. c) Charge stored at $CuWO_4$ surface calculated from current transients after turning off the light (black squares) and Gaussian fitting of the charge (red dash).

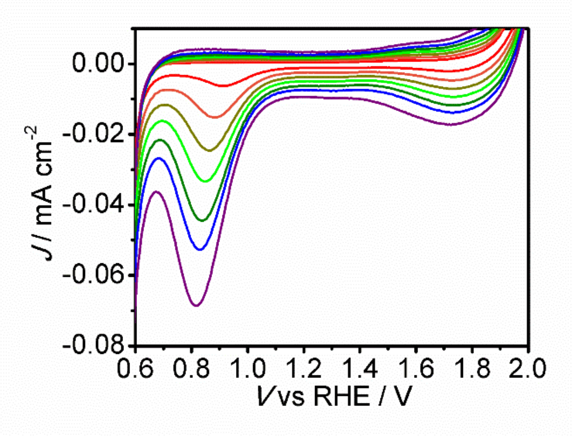

Figure S6. CV taken after holding potential at 2.3 V vs RHE for 60 s in the dark. Scan rates varies from 200, 400, 600, 800, 1000, 1200 and 1500 mV s^{-1} corresponding to red, orange, dark yellow, green, dark green, blue and purple solid. The peak intensity after the dark pretreatment is slightly smaller compared to the light pretreatment.

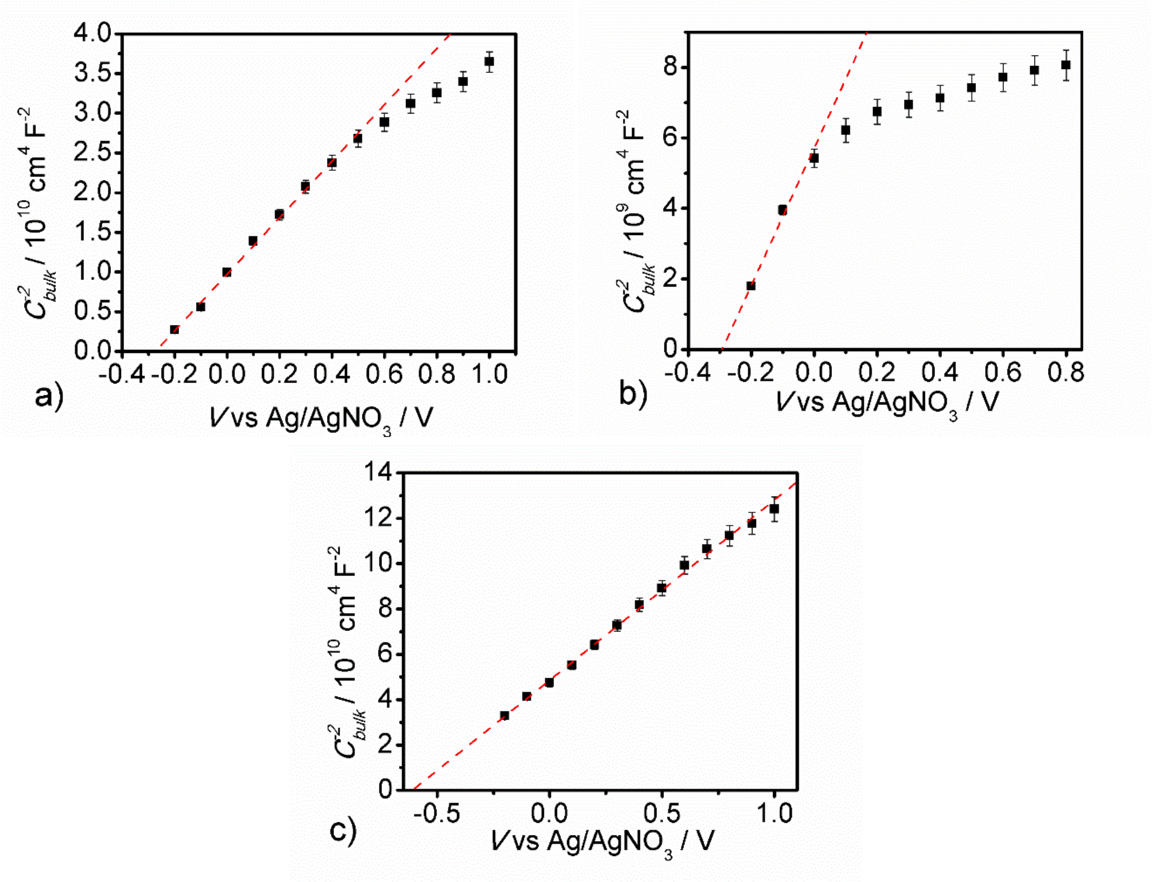

Figure S7. Mott-Schottky plots (black scattered points) and linear fit (red dash) of $CuWO_4$ in a) MeCN electrolyte, b) MeCN electrolyte containing 2% H_2O, and c) dichloromethane electrolyte.

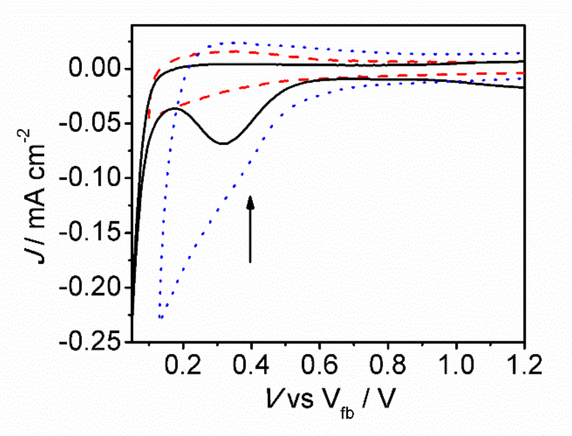

Figure S8. CV after holding potential at ~1.8 V vs V_{fb} for 60 s in the dark, measured in H_2O (black solid), MeCN (red dash) and MeCN with 2% H_2O (blue dot). Scan rate is 1500 mV s^{-1}.

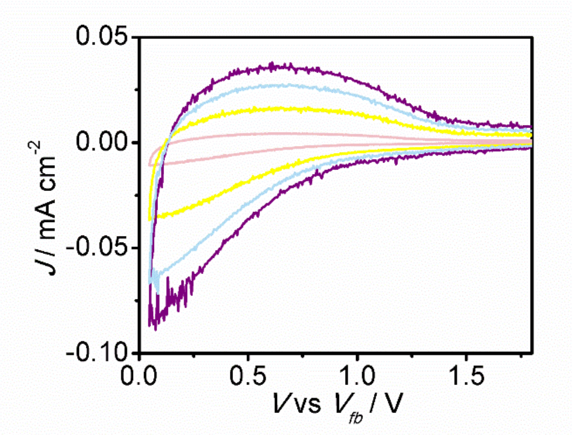

Figure S9. CV after holding potential at ~1.8 V vs V_{fb} for 60 s in the dark, measured in 0.2 M $TBAPF_6$ in dichloromethane in the glovebox. Scan rates varies from 200, 800, 1500 and 2000 mV / s corresponding to pink, yellow, cyan and purple solid lines. Initial scan is in the cathodic direction.

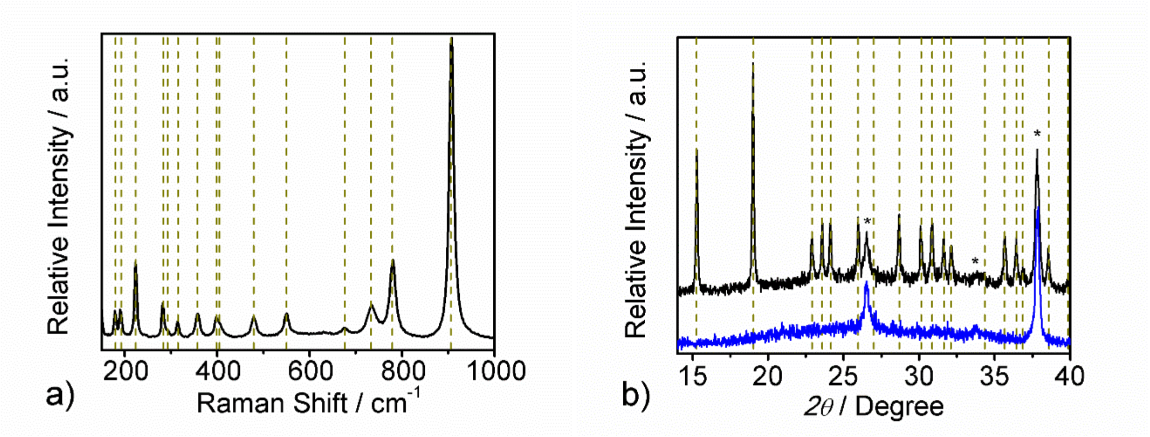

Figure S10. a) Raman spectrum and b) XRD pattern of $CuWO_4$ synthesized by spray pyrolysis and annealed at 550 °C for 1 hr (SP-$CuWO_4$). Experimental data of $CuWO_4$ are shown as black curves and peak positions from literature are shown as vertical dark yellow dash. The XRD pattern of FTO substrate is shown as blue curve as control experiment, and the diffraction peaks from FTO are labeled as *.

As shown in Figure S10, the resulted SP-$CuWO_4$ films show Raman and XRD peaks corresponding to $CuWO_4$ peaks in literature[7–9], apart from those from the underlying FTO substrate marked as * in XRD pattern. These results confirm the pure $CuWO_4$ composition of the resulted films.

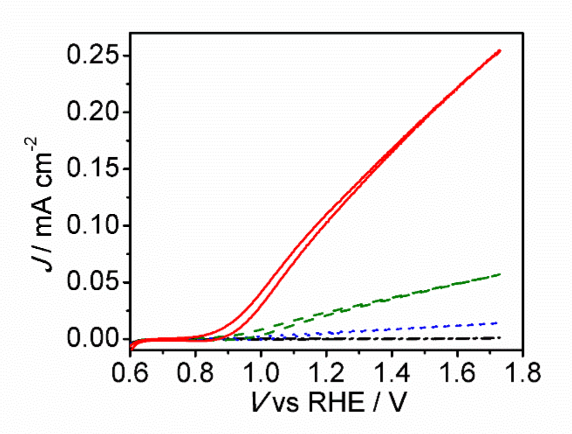

Figure S11. *J-V* curves of SP-$CuWO_4$ under 1 sun (red solid), 0.33 sun (green dash), 0.1 sun (blue dots) illumination and in the dark (black dash dot) measured in pH 9 aqueous (H_2O) electrolyte.

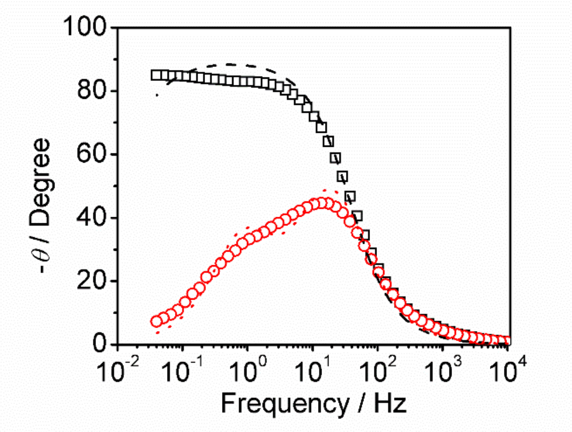

Figure S12. Bode phase plots of SP-$CuWO_4$ at 0.93V vs RHE in the dark (black squares) and under 1 sun illumination (red circles) measured in pH 9 aqueous (H_2O) electrolyte. Fitting curves are shown as black dash and red dots for dark and 1 sun measurements, respectively.

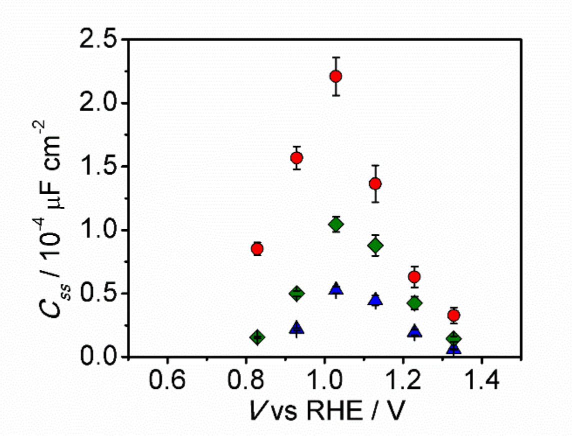

Figure S13. C_{ss} obtained from fitting EIS measured in pH 9 aqueous (H_2O) electrolyte under 0.1 sun (blue triangles), 0.33 sun (green diamonds) and 1 sun (red circles) illumination with SP-$CuWO_4$.

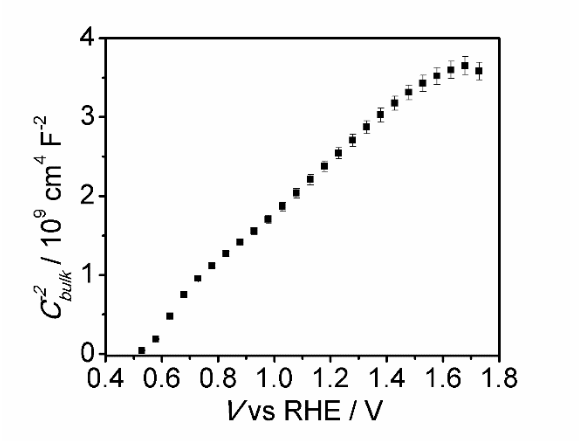

Figure S14. Mott-Schottky plots of SP-$CuWO_4$ measured in the dark in pH 9 aqueous (H_2O) electrolyte.

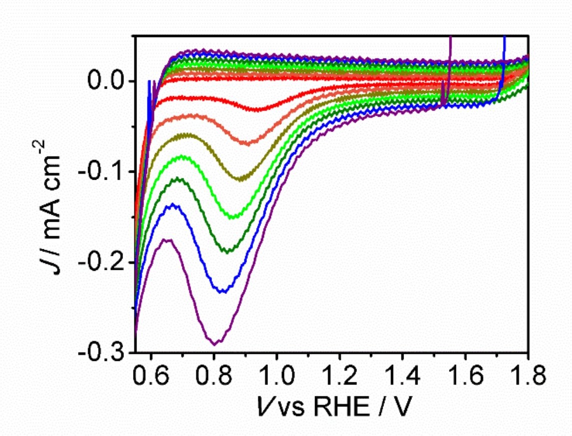

Figure S15. CVs taken after holding potential at 2.3 V vs RHE for 60 s under 1 sun illumination at scan rates from 200, 400, 600, 800, 1000, 1200 and 1500 mV s^{-1} corresponding to red, orange, dark yellow, green, dark green, blue and purple. Experiment was conducted in pH 9 aqueous electrolyte.

As shown in Figure S11, the *J*-*V* curves of SP-$CuWO_4$ measured under illumination for water oxidation show an onset potential of 0.85 - 0.90 V vs RHE, depending on the light intensity. The photocurrent at 1.23 V vs RHE under 1 sun illumination is ~0.13 mA cm^{-2}, which is similar as reported values.[1,3,10,11] In Figure S12, the EIS data show two capacitive features in the Bode phase plot under 1 sun illumination, while only one is observed in the dark. The surface state capacitance, C_{ss}, increases with increasing light intensity, as shown in Figure S13. These facts suggest that the surface state of SP-$CuWO_4$ is light-induced, rather than intrinsic. The Mott-Schottky plot measured in the dark in Figure S14 shows no Fermi level pinning, further confirming that the surface state is not present in the dark. Lastly, the CV surface measurement in Figure S15 shows a capacitive peak around 0.9 V vs RHE, the peak position of which shifts negatively with increasing scan rate, while its peak current increases. This peak position is close to that of C_{ss} in Figure S13, and matches with water oxidation onset potential, which is essentially the same observation with $CuWO_4$ synthesized via ALD. Therefore, we conclude that the role of surface state as water oxidation intermediate is general for $CuWO_4$, rather than specifically limited to our electrode made by ALD.

References

(1) Gao, Y.; Zandi, O.; Hamann, T. W. Atomic Layer Stack Deposition-Annealing Synthesis of $CuWO_4$. *J. Mater. Chem. A* **2016**, *4*, 2826–2830.

(2) Liu, R.; Lin, Y.; Chou, L. Y.; Sheehan, S. W.; He, W.; Zhang, F.; Hou, H. J. M.; Wang, D. Water Splitting by Tungsten Oxide Prepared by Atomic Layer Deposition and Decorated with an Oxygen-Evolving Catalyst. *Angew. Chemie Int. Ed.* **2011**, *50*, 499–502.

(3) Lhermitte, C. R.; Bartlett, B. M. Advancing the Chemistry of $CuWO_4$ for Photoelectrochemical Water Oxidation. *Acc. Chem. Res.* **2016**, *49*, 1121–1129.

(4) Arora, S. K.; Mathew, T. Dielectric Studies of $CuWO_4$ Crystals. *Phys. Stat. Sol.* **1989**, *116*, 405–413.

(5) Bisquert, J. Chemical Capacitance of Nanostructured Semiconductors: Its Origin and Significance for Nanocomposite Solar Cells. *Phys. Chem. Chem. Phys.* **2003**, *5*, 5360–5364.

(6) Bisquert, J. Physical Electrochemistry of Nanostructured Devices. *Phys. Chem. Chem. Phys.* **2008**, *10*, 49–72.

(7) Kihlborg, L.; Gebert, E. $CuWO_4$, a Distorted Wolframite-Type Structure. *Acta Crystallogr. Sect. B Struct. Crystallogr. Cryst. Chem.* **1970**, *26*, 1020–1026.

(8) Ruiz-Fuertes, J.; Errandonea, D.; Segura, A.; Manjón, F. J.; Zhu, Z.; Tu, C. Y. Growth, Characterization, and High-Pressure Optical Studies of $CuWO_4$. *High Press. Res.* **2008**, *28*, 565–570.

(9) Ruiz-Fuertes, J.; Sanz-Ortiz, M. N.; González, J.; Rodríguez, F.; Segura, a; Errandonea, D. Optical Absorption and Raman Spectroscopy of $CuWO_4$. *J. Phys. Conf. Ser.* **2010**, *215*, 12048.

(10) Pyper, K. J.; Yourey, J. E.; Bartlett, B. M. Reactivity of $CuWO_4$ in Photoelectrochemical Water Oxidation Is Dictated by a Midgap Electronic State. *J. Phys. Chem. C* **2013**, *117*, 24726–24732.

(11) Yourey, J. E.; Bartlett, B. M. Electrochemical Deposition and Photoelectrochemistry of $CuWO_4$, a Promising Photoanode for Water Oxidation. *J. Mater. Chem.* **2011**, *21*, 7651–7660.